ARTÍCULO EN PRENSA

Revista de Teledetección. 2006. 26: 66-76

Atmospheric correction algorithm for POLDER data.Case study: DAISEX 1999 campaign

R. Pedrós[1], J.A. Martínez-Lozano[1], J. Moreno[2], M.P. Utrillas[1], J.L. Gómez-Amo[1]

[1] Grupo de Radiación Solar, Universitat de València, Spain.
[2] Laboratorio de Observación de la Tierra, Universitat de València, Spain.

Universitat de València
Departament de Física de la Terra i Termodinàmica
c/ Dr. Moliner 50, 46100 Burjassot, Valencia. Spain

ABSTRACT

This paper presents an algorithm to correct the effects of the atmosphere of POLDER hyperspectral and multiangular reflectance, paying particular emphasis to the aerosol effect. The data were acquired during the European Space Agency campaign DAISEX-99. The algorithm is based on the inversion of measured reflectance in two steps. First, we invert the POLDER reflectances to determine the three parameters of a bidirectional reflectance distribution function (BRDF) of the surface. These values are the first guess of the surface parameters for the second step. In the second step, we invert again the reflectance to obtain three surface parameters and four aerosol variables, in rural sites, and five variables in the rest. The aerosol variables are the particle density of the basic aerosol components: water-insoluble, water soluble and soot particles, sea-salt in accumulation mode and sea-salt in coarse mode. Thus, the algorithm output is the content of some aerosol basic components and the BRDF parameters of the surface. Applying the Mie scattering theory we have obtained the aerosol optical depth (AOD) of the retrieved aerosols and compared it with the values obtained from ground-based solar irradiance extinction measurements. The available information about the aerosols coming from airmass backtrajectories and isobaric maps provides a boundary condition for the inversion. Using this information we show that the AOD values are closer to the measured values and thus the performance of the algorithm is betterl.

KEY WORDS: atmospheric correction; aerosols; aerosol optical depth; POLDER; DAISEX; hyperspectral; multiangular.

RESUMEN

Este artículo presenta un algoritmo para corregir los efectos de la atmósfera de la reflectividad multiangular e hiperespectral de POLDER, prestando especial atención al efecto de los aerosoles. Los datos fueron adquiridos durante la campaña DAISEX-99 de la Agencia Espacial Europea. El algoritmo está basado en la inversión de la reflectividad medida en dos pasos. Primero, se invierte la reflectividad de POLDER para determinar los tres parámetros de la función de distribución de la reflectividad bidireccional de la superficie (BRDF). Estos valores son los datos de entrada de la superficie para el segundo paso. En este segundo paso, invertimos de nuevo la reflectividad para obtener tres parámetros de la superficie y cuatro parámetros de los aerosoles para localidades rurales y cinco en el resto. Los parámetros de los aerosoles son la densidad de partículas de los componentes básicos de los aerosoles: insoluble en agua, soluble en agua, hollín, sales marina es modo de acumulación y sales marinas en modo grueso. Por tanto, la salida del algoritmo es el contenido de varios componentes básicos y los parámetros del modelo de BRDF. Aplicando la teoría de dispersión de Mie hemos obtenido el espesor óptico de los aerosoles (AOD) y comparado el resultado con los valores determinados a partir de medidas de extinción de la radiación solar a nivel del suelo. Se ha obtenido como condición de contorno para la inversión la información disponible sobre los aerosoles obtenida a partir de las retrotrayectorias de las masas de aire. Utilizando esta información mostramos que los valores del AOD están más próximos a la medida y que por tanto el funcionamiento del algoritmo es mejor.

PALABRAS CLAVE: corrección atmosférica; aerosoles; espesor óptico de aerosoles; POLDER; DAISEX; hiperespectral; multiangular.

INTRODUCTION

The DAISEX campaign, involved simultaneous data acquisitions using three different airborne imaging spectrometers over test sites in southeast Spain (Barrax) and the Upper Rhine valley (Colmar, France, and Hartheim, Germany) (ESA, 2001a). The main scientific objectives of DAISEX,

funded by the European Space Agency (ESA), were to demonstrate the retrieval of geo/biophysical variables from imaging spectrometer data. Target variables included surface temperature, leaf area index, canopy biomass, leaf water content, canopy height, canopy structure, and soil properties (Berger et al., 2001). To retrieve such variables it is vital to obtain accurately surface reflectance. The objective of the atmospheric correction is to retrieve surface reflectance from remotely sensed imagery by removing atmospheric effects. Currently, atmospheric aerosols are the main cause of uncertainty in atmospheric correction methods. Season and location are only partial predictors of aerosol optical properties, because aerosol size, for instance, can vary significantly from day-to-day at a single location (Holben et al., 1996; Remer et al., 1998). Such day-to-day variation stems from meteorological variability rather than direct changes in the strength of aerosol sources. Aerosol optical properties are particularly dependent on the air mass residence times and the duration of stagnant conditions (Remer et al., 1999). In order to obtain the maximum amount of information from satellite measurements, a major effort in atmospheric correction is underway for retrieval of atmospheric aerosols parameters that will facilitate atmospheric corrections (Kaufman and Tanré, 1996; Kaufman et al., 1997; Santer et al., 1997).

The DAISEX campaigns involved the use of DAIS-7915 and HyMap^{TM} imaging spectrometers operating simultaneously from the same aircraft (DLR Dornier 228). In addition, the French ARAT aircraft flew over the site during the 1999 campaign with two instruments onboard, the LEANDRE Atmospheric Lidar and the POLDER imaging radiometer. The campaign took place during the summers of 1998, 1999 and 2000 in Barrax (Spain) and Colmar (France). Both DAIS/HyMap and POLDER flights provided a valuable database of hyperspectral and multiangular data. In addition, several instruments were deployed at ground level to validate the retrieval of geo/biophysical variables (Berger et al., 2001). At the same time a spectroradiometer LI-COR 1800 was used to measure the direct spectral irradiance at the ground level, which was used to obtain the aerosol optical depth (hereafter AOD). In a first step, the acquired hyperspectral and multiangular data were used by applying an atmospheric correction algorithm that considered a Lambertian surface and a simple approach for the aerosols (ESA, 2001a). This paper intends to improve the analysis of the data by presenting a new algorithm specifically developed to correct atmospherically hyperspectral and multiangular data, which considers a non-Lambertian surface and a more accurate treatment of the aerosols. The algorithm output was compared with the retrieved AOD.

THE ATMOSPHERIC CORRECTION ALGORITHM

LLand surface and atmosphere are coupled to each other over a variety of time scales through the exchanges of water, energy and carbon. One of the main consequences of this coupling is that the measurement of the light reflected by the land surface is affected by the multiple scattering and absorption by the atmospheric components. To remove the contribution due to the scattering of the atmosphere the usual procedure is to consider that the atmosphere can be described by using standard conditions, particularly regarding to the aerosols (ESA, 2001a). These atmospheric standard conditions are included in a radiative transfer code that solves the Radiative Transfer Equation (RTE) following an inversion procedure. This procedure consists in modifying the atmospheric parameters in order to reproduce the measured reflectance, either solving each time the RTE or building a look-up table. This approach might lead to errors when the atmosphere is particularly unstable or when the aerosols are a mixture of different types of aerosols, which is often the case (Pedrós, 2001). On the other hand, the surface is often considered lambertian in order to simplify the approach (ESA, 2001a), which is limiting.

Several techniques can be applied in inverse problems, for instance neural networks. Neural networks are capable of approximating non-linear inverse functions and of processing efficiently large amounts of data. Jamet et al. (2004) used it to retrieve aerosol optical properties from SeaWiFS images and Schroeder et al. (2002) developed an algorithm to correct MERIS data. The neural networks are trained using radiative transfer computations for very different atmospheric conditions. This tries to overcome the ill-posed problem by building a database with very different situations.

We propose here a simple procedure to invert based on the minimization of a merit function in two steps. A flow diagram of the inversion is shown in Fig. 1.

Step 1

First, we select a set of pixels from an image where we can identify the type of surface. The surface can be identified if the spatial resolution is suitable to apply pattern recognition techniques, for example. A spatial resolution of 50x50 m would be

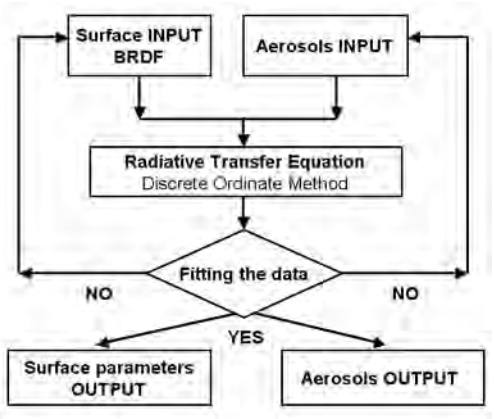

Figura 1. Flow diagram of the algorithm.

sufficient (ESA, 2001b). For these pixels we retrieve the three parameters of the bidirectional reflectance distribution function (BRDF) model of Rahman-Pinty-Verstraete (RPV) (Rahman et al., 1993), assuming a standard atmosphere: mid-latitude summer atmosphere, rural aerosols with visibility 23 km. In the RPV model the surface is described using three parameters ($?_0$, g, and k) for each wavelength. The parameter $?_0$ characterizes the reflectance of the surface cover, the parameter g is the Henyey-Greenstein asymmetry factor, ranging from -1 to +1, and k indicates the level of anisotropy of the surface. The retrieved RPV values will probably not be correct but if we have identified the type of surface, we can check if they are reasonable. These values will be used as boundary conditions for the surface in step 2.

The PRV parameters are retrieved by minimizing the merit function F,

$$F = \sqrt{\sum \left(R_{POL} - R_{MOD}\right)^2} + \mathrm{P} \qquad (1)$$

were R_{POL} are the POLDER reflectances, R_{MOD} the modeled reflectances using MODTRAN4 radiative transfer code (Air Force Research Lab, 1999), and P is a penalty term, which is added to the merit function when the inverted parameters take incongruous values. To minimize F we have applied the Nelder-Mead Simplex optimization algorithm that consists in moving across the called Weighted Sum of Squares (WSS) surface to reach the global minimum without knowing ahead of time the shape of this WSS surface. If the model has m parameters, the WWS will be represented as an m-dimension surface. The method constructs a simplex, a shape with m+1 points, where m is the number of parameters by using a starting point or first guess values. The program calculates the WSS at each point of the simplex on the WSS surface. The simplex moves over the WSS surface and contracts around the global minimum, i.e. the solution. We have chosen this numerical method because it shows great stability and converges quickly.

Step 2

We carry out another minimization of the merit function, this time using M+3 model parameters: three parameters to describe the RPV model of the surface and number M parameters to describe more accurately the aerosol type and content. The first guess of the RPV values are the outcome of the first step, and we have to determine what is the number M of aerosol parameters required and what would be a first guess of them.

In order to describe accurately the aerosols, we have used the OPAC database (Hess et al., 1998). The OPAC database considers 10 different types of aerosols or basic components: water-insoluble, water-soluble, soot, sea salt in accumulation mode, sea salt in coarse mode, mineral in nuclei mode, mineral in accumulation mode, mineral in coarse model, mineral-transported and sulfate. The water-insoluble are mostly soil particles with a certain amount of organic material. The water-soluble aerosols consist in various kinds of sulfates, nitrates and other organic substances. These sulfates are often used to describe anthropogenic aerosols. The soot aerosols represent absorbing black carbon. Sea-salt particles consist in the various kinds of salt contained in sea-water. Two sea-salt models are considered to allow for a different wind-speed-dependent increase of particle number for particles of different size. Mineral aerosols are used to represent the desert dust, a mixture of quartz and clay minerals, and it's modeled with three modes to allow to consider increasing relative

amount of large particles for increasing turbidity. Mineral transported are used to describe desert dust that is transported over long distances. The sulfate aerosols (75% of H_2SO_4) are used to describe the amount of sulfate found in the Antarctic aerosols and to represent the stratospheric background. OPAC include 10 pre-defined aerosol models by taken up to five basic components and their corresponding particle densities: continental clean, continental average, continental polluted, urban, desert, maritime clean, maritime polluted, maritime tropical, Arctic and Antarctic. We notice that excluding desert aerosols, Arctic and Antarctic, the aerosol models only require five components: water-insoluble, water-soluble, soot, sea-salt in accumulation mode and sea-salt in coarse mode. Arctic and Antarctic aerosols are obviously discarded in our measurement area, as well as desert aerosols, because there wasn't any Saharan dust intrusion during the days of the POLDER flights (Pedrós et al., 2003). OPAC enables the user to create his own aerosol model by choosing up to five basic aerosol components and its particle densities, assuming that the aerosols are spherical particles in an external mixture, i.e. particles from different sources remain separated. Therefore, the number M of parameters to describe the aerosols is five, that corresponds to the particle density of the basic aerosol components water-insoluble, water-soluble, soot, sea-salt in accumulation mode and sea-salt in coarse mode. We will minimize the merit function in Eq. 1, but now R_{MOD} depends on 8 parameters.

The remaining question is what the first guess values for the aerosols are. We could take the aerosol components and its particle densities from any of the pre-defined models. However, to avoid a possible biased first guess that could influence the results, we have considered a mixture between the OPAC pre-defined models continental, maritime and urban, a kind of average aerosols. The OPAC database contains an implementation of the Mie scattering that allows the calculation of the AOD, the phase function, the asymmetry factor, the scattering and the absorption coefficients. These calculated aerosol parameters have been introduced in MODTRAN4, to obtain an accurate description of the aerosols in the radiative transfer calculations. The MODTRAN4 options used were: User-defined scattering phase functions (cards 3B1, 3B2 and 3C1-3C6) and User-defined aerosol parameters (2D2). For a more accurate description of the multiple scattering, a number of 16 streams were considered, though it increased remarkably the calculation time.

The result of this eight-parameter inversion allows obtaining the three parameters of the surface and the five parameters of the aerosols, at the same time. The aerosol parameters that correspond to selected pixels can be used to correct atmospherically the image as we can reasonably assume that the atmosphere is constant for the whole image.

MATERIAL AND METHODS

We have applied the algorithm to a case study: the ARAT flight over Barrax at 12:00 GMT on 3 June 1999. During this flight, POLDER data were acquired in nine channels (0.443, 0.500, 0.550, 0.590, 0.670, 0.700, 0.720, 0.800, 0.864 ?m) for 7 or 9 observation angles (azimuth observation, in addition to 3 or 4 symmetric angles up to about 45 degrees from the vertical). More details about POLDER instrument can be found in Deschamps et al. (1994). We have compared the algorithm output for the aerosols with the aerosol properties retrieved from the measurements carried out with the spectroradiometer LI-COR 1800. Due to the availability of instrumentation during the campaign we can only retrieve the AOD. The AOD is a good indicator of the aerosol burden and its spectral distribution, though so far it didn't allow a description of the aerosol composition (Pedrós et al., 2003). Therefore we have restricted the comparison to AOD because it represents well the aerosol burden and we are going to obtain information about the aerosol composition.

With the spectroradiometer LI-COR 1800 we measured the direct spectral irradiance in the range [300, 1100] nm. The instrument has a band pass of 6 nm and a step of 1 nm. The entrance optics is Teflon dome with a collimator with a FOV of 5º. The spectroradiometer is provided with a simple monochromator and the sensor element is a silicon photodiode. The instrument accuracy, relative to the NIST standard is 3-10% depending on the wavelength, with a value of about 5% in the visible range. The total atmospheric optical depth, $\tau_{T\lambda}$ is determined from the spectral irradiance measurements at normal incidence using the Beer-Lambert exponential law. This total optical depth can be expressed, in the visible range, as the sum of the optical depths related to the different atmospheric components:

$$\tau_{T\lambda} = \tau_{R\lambda} + \tau_{a\lambda} + \tau_{O\lambda} + \tau_{w\lambda} + \tau_{N\lambda} \quad (2)$$

where $\tau_{R\lambda}$ is the molecular scattering optical depth (which is usually calculated using the Rayleigh approximation), $\tau_{a\lambda}$ is the aerosol extinction optical depth (AOD), and $\tau_{O\lambda}$ $\tau_{w\lambda}$ and $\tau_{N\lambda}$ are the optical depth due to O_3, H_2O and NO_2 absorption respectively. Once the total atmospheric optical depth is determined, the AOD can be obtained by eliminating contributions due to Rayleigh scattering and to absorption by other atmospheric components from the total transmittance. In this case, although our spectral irradiance measurements ranged from 300 to 1100 nm, we limited the study of the spectral AOD to the 400-670 nm band, where the only components showing non-negligible absorption are ozone (Chappuis band) and NO_2. In this way, the errors introduced by all the other atmospheric constituents in the parameterization of the AOD are eliminated. The absorption due to NO_2 has not been considered due to the rural characteristics of the measurement site. However the correction due to ozone is necessary since the optical depth of ozone in the Chappuis band represents, on average, 8% of the total atmospheric optical depth. This value depends on the wavelength, being only 4% at 500 nm.

To determine $\tau_{T\lambda}$ we used the values of the extraterrestrial spectrum proposed by the SMARTS2 model (Gueymard, 2001), smoothing the data to the band pass of our spectroradiometer. For the air mass, the empirical expression proposed by Kasten and Young (1989) was used. The Rayleigh optical depth was calculated from the approximation of Bodahine et al. (1999). The ozone absorption coefficients from Anderson and Mauersberger (1992) were assumed and the total ozone amount was retrieved from the ozone soundings performed by the Spanish National Meteorological Institute. The accuracy of this technique to retrieve AOD was proved with a comparison with the results obtained with the LEANDRE Lidar that was also on the same plane than POLDER (Martinez-Lozano et al., 2002).

RESULTS AND DISCUSSION

In a general case, we do not know *a priori* either what kind of surfaces we have to use for the selected pixels, or the number of wavelengths for the development of the algorithm. In principle, the algorithm should be applied to different surfaces and for as much as possible spectral channels. Some tests (not shown here), made us conclude that we obtain a better result if we only use bare soil. The reason is probably that in vegetation surfaces some other external factors, that haven't been considered in the variables to invert, vary the reflectance, e.g. the inclination of the leave due to the sun position. Regarding to the number of wavelengths, we have taken the nine POLDER channels, though the algorithm is quite expensive in calculation time. The advantage of these channels is that avoid some important absorption bands, although MODTRAN4 includes the state-of-the-art treatment of the gas absorption by using the HITRAN database (Rothman et al., 1998). From the 7 to 10 POLDER observation angles we will use 7 as it was the number recommended to obtain the maximum information about the surface (ESA, 2001b).

The inverse problems are typically ill-posed, which means that the solution is not unique. In other words, different sets of values of the model parameters correspond to the same values of the observed data. Therefore, *a priori* we cannot know which solution is the correct one, i.e. the one that corresponds to reality. We suggest a possibility and evaluated the results. We propose to use the available information to obtain a first guess of the aerosols as closer to the reality as possible.

The step 1 of the algorithm has been applied to retrieve the RPV parameters for the soil pixels, assuming that the aerosols are standard for our measurement site (rural aerosols, visibility 23 km). We apply the algorithm to invert the POLDER data. The retrieved RPV values are in Table I. These values are probably not correct because they have retrieved using a rough model for the aerosols. Nevertheless, as we know that we are dealing with bare soil, we know that they are reasonable. These values are a boundary condition for the surface in the inversion of step 2. Regarding to the aerosols, we are going to compare the values when we set the first guess values using average aerosols and when using the available information about the aerosols.

Inversion using average aerosols

We have considered a mixture between the OPAC pre-defined continental, maritime and urban models, a kind of average aerosols. The particle densi-

λ (μm)	ϱ_0	g	k
0.443	0.027	-0.216	0.784
0.500	0.041	-0.217	0.731
0.550	0.056	-0.217	0.738
0.590	0.093	-0.217	0.672
0.670	0.117	-0.210	0.715
0.700	0.183	-0.202	0.593
0.720	0.278	-0.184	0.618
0.800	0.280	-0.154	0.739
0.864	0.309	-0.147	0.802

Table I. Input BRDF parameters for the RPV BRDF model for step 2 in the inversion, resulting from step 1.

ties of the basic components appear in Table II. For water-insoluble is 0.15 particle cm^{-3} that corresponds to continental clean. The water-soluble value of 1600 particle cm^{-3} corresponds to maritime clean. The soot value is 2500 particle cm^{-3}, halfway between maritime polluted (5000 particle cm^{-3}) and maritime clean (0, i.e. no soot). The values for sea-salt in accumulation mode and in coarse mode are halfway between maritime clean and maritime polluted (20 and 3.2e-3, respectively) and urban and continental (both 0, i.e. no sea-salts). Figure 2 shows the comparison between the measured and the algorithm output reflectances. The POLDER reflectances are well retrieved, having a relative mean bias deviation (RMBD) of less than 1% for all wavelengths, except at 0.443 μm with a RMBD around 15%, particularly due to the differences at great view zenith angles. The explanation could be an underestimation of the aerosol contribution in MODTRAN4 for such conditions. Nevertheless, the retrieved AOD underestimates the measured one, with a RMBD of –93.4% (see Fig. 3). Table I shows the RPV input parameters and Table III the output ones. The input and output reflectances of the surface (ϱ_0) are quite similar at all wavelengths. The Henyey-Greenstein asymmetry factor (g) changes particularly in the visible range between the input and the output, but the main differences appear in the anisotropy of the surface (k).

The output particle densities are in Table II. The input and output particle densities of water-soluble aerosols are very similar. On the other hand, the algorithm retrieves almost no insoluble particles and sea-salts but more soot particles than the input value. The combination of only soot and water-soluble particles it only appears in polluted maritime aerosols, but always associated to sea-salt particles (Hess et al., 1998). Thus, although the retrieved reflectances are very close to the measurements, the solution corresponds to unlikely existing aerosols. This fact would explain the discrepancies between the algorithm and the measured AOD shown in Fig. 3.

Basic component	Input particle density (part cm^{-3})	Output particle density (part cm^{-3})
water-insoluble	0.15	0.0018
water-soluble	1600	1577
soot	2500	3626
sea salt in accumulation mode	10	2.2e-4
sea salt in coarse mode	1.6e-3	2.0e-4

Table II. Input and output aerosol basic components and its particle density for an average aerosol model.

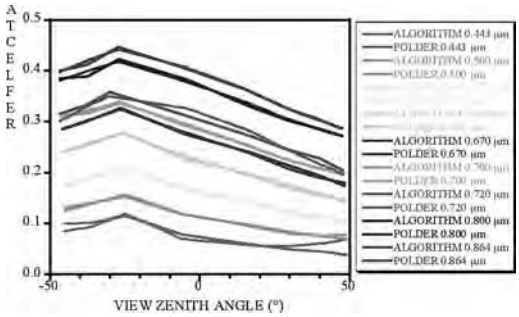

Figure 2. POLDER Reflectance (full line) and algorithm reflectance (dotted line) over bare soil using average aerosols. Flight at 12:00GMT on 3 June 1999.

λ (μm)	ϱ_0	g	k
0.443	0.0099	-0.6864	0.0470
0.500	0.0337	-0.4630	0.3597
0.550	0.0627	-0.3643	0.4475
0.590	0.1258	-0.3211	0.3665
0.670	0.1502	-0.2785	0.4787
0.700	0.2422	-0.2628	0.3779
0.720	0.4337	-0.2384	0.5838
0.800	0.3628	-0.1957	0.5772
0.864	0.3879	-0.1842	0.6738

Table III. Output RPV BRDF parameters for bare soil, using average aerosols.

Inversion using available information

We have used the NOAA ARL HYSPLIT4 model backtrajectories, which are easily accessible on-line in NOAA (2004), to set the first guess of the aerosols. More details about the HYSPLIT4 model can be found in Draxler (1999).

Fig. 4 shows the HYSPLIT4 backtrajectory for the 3 June 1999 ending at 12:00 GMT. We can see from Fig. 4 that the airmasses come from the Atlantic Ocean but they have swept the Iberian Peninsula. Thus, we can reasonably consider that the aerosols could be a mixture of continental and maritime aerosols. Valuable information we can use is that the study site is in a rural area. Thus we can reduce in one parameter the inversion by removing soot from the aerosol basic components, as it is only present in polluted areas.

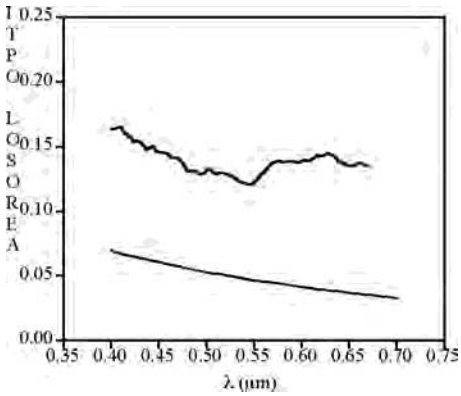

Figure 3. Measured (full line) and algorithm retrieved (dotted line) values for the aerosol optical depth using average aerosols on 3 June 1999 at 12:00GMT.

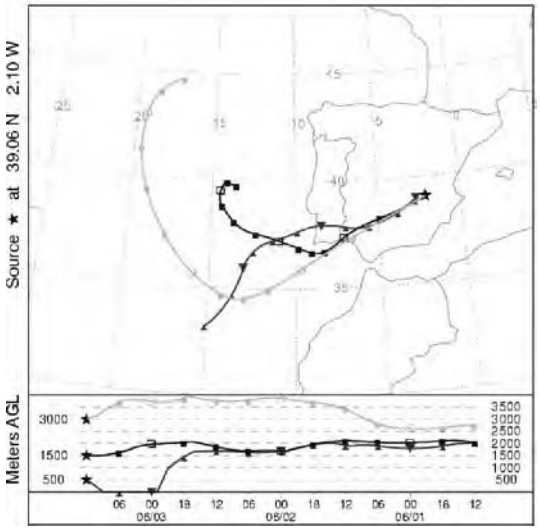

Figure 4. Three-day back-trajectories computed with HYSPLIT4 ending at 12:00 GMT on 3 June 1999.

We have also used information coming from isobaric maps provided by the Spanish National Meteorological Institute (Fig. 5). We can see in Fig. 5 that the meteorological conditions are dominated by the passing of a cold front, which is located over the western third of the Iberian Peninsula at 12:00 GMT two days before the flight. This cold front cleared the atmosphere due to precipitation scavenging of aerosols.

Therefore, the aerosols could probably be made of water-insoluble, water-soluble, sea-salt in accumulation mode and sea-salt in coarse mode particles. Due to the clear conditions, we have used the particle densities for water-insoluble and water-soluble of the continental clear OPAC model (0.15 and 2600 particles cm^{-3} for insoluble and soluble, respectively), and for sea-salt particles we have used the values that are common for maritime clean and maritime polluted (20 and 3.2e-3 particles cm^{-3} for accumulation and coarse modes, respectively). These values are used to set the first guess of the aerosol and are shown in Table IV.

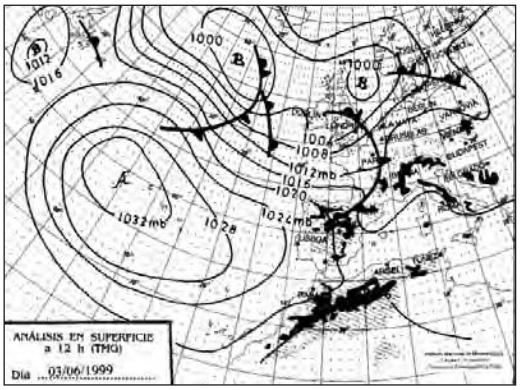

Figure 5. Surface isobaric map at 12:00 GMT on 3 June 1999. Source: Spanish National Meteorological Institute.

Basic component	Input particle density (part cm^{-3})	Output particle density (part cm^{-3})
water-insoluble	0.15	0.01
water-soluble	2600	2596
sea salt in accumulation mode	20	19
sea salt in coarse mode	3.2e-3	3.3e-2

Table IV. Aerosol input basic components and its particle density using the available information about the aerosols.

The POLDER and algorithm reflectances again are very close (compare Fig. 6 and Fig. 2) with a RMBD less that 1%, except for 0.443 μm when is around 15%. But in this case, the algorithm AOD is very close to the measured AOD (see Fig. 7) with a RMBD of 1%. The input and output particles densities shown in Table IV mean that the algorithm retrieves maritime aerosols in very clean conditions. Therefore, the algorithm has retrieved only maritime aerosols, although the first guess that was a mixture of continental and maritime aerosols.

The output RPV variables are in Table V. One can see that the values for ϱ_0, g and k are very similar to those of Table III, using average aerosols, due to the fact that both cases have the same first guess of the of ϱ_0, g and k (Table I).

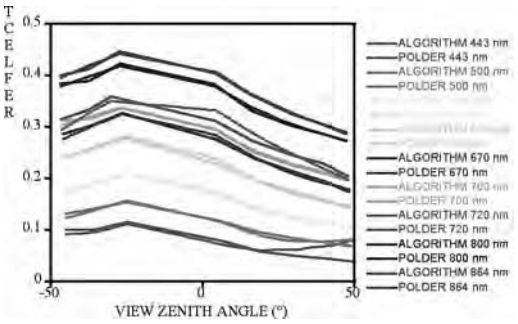

Figure 6. POLDER Reflectance (full line) and algorithm reflectance (dotted line) over bare soil using the available about the aerosols. Flight at 12:00GMT on 3 June 1999.

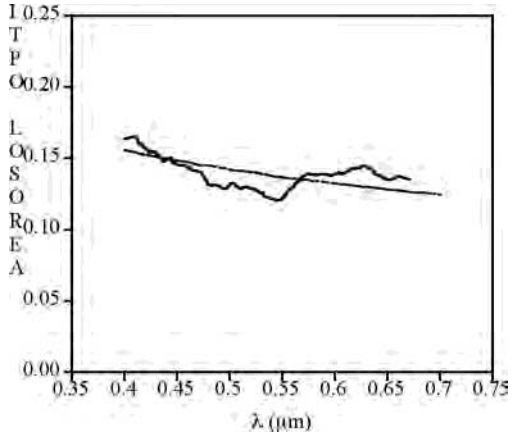

Figure 7. Measured (full line) and algorithm (dotted line) aerosol optical depth using the available information about aerosols on 3 June 1999 at 12:00GMT.

Other aerosol optical properties

Applying the Mie theory we have obtained the extinction coefficient (Fig. 8a), the phase function (Fig. 8b), the asymmetry factor (Fig. 8c) and the absorption coefficient (Fig. 8d). These optical properties have been used in the user-defined aerosol properties in MODTRAN4. Unfortunately these properties cannot be retrieved from the measurements acquired during the DAISEX campaign. The retrieval of these aerosol properties requires additional measurements at several angles of the sky radiance in the solar almucantar plane, normal to the solar principal plane (Nakajima, 1996). These measurements were carried out with a high precision Optronic 754-O-PMT in the measurement site during the campaign DAISEX 2000, when POLDER instrument was not available. The sky radiance signal is so low that we used a telescope in the entrance optics, in addition to the instrument photomultiplier in the detection. The analysis of the data acquired during DAISEX 2000 can be found in Pedrós (2001). The Solar Radiation Group of Valencia has recently acquired two photometers Cimel allowing an automatic measurement of the sky radiance that could be used in future ESA-funded campaigns to validate the retrieval of optical properties shown in Fig. 8.

λ (μm)	ϱ_0	g	k
0.443	0.0086	-0.6569	0.0478
0.500	0.0264	-0.5036	0.3429
0.550	0.0548	-0.3783	0.5247
0.590	0.1112	-0.3493	0.4027
0.670	0.1399	-0.2976	0.5315
0.700	0.2343	-0.2778	0.3770
0.720	0.4330	-0.2529	0.5975
0.800	0.3590	-0.2239	0.5225
0.864	0.3982	-0.2096	0.6097

Table V. Output RPV BRDF parameters for bare soil, using the available information about aerosols.

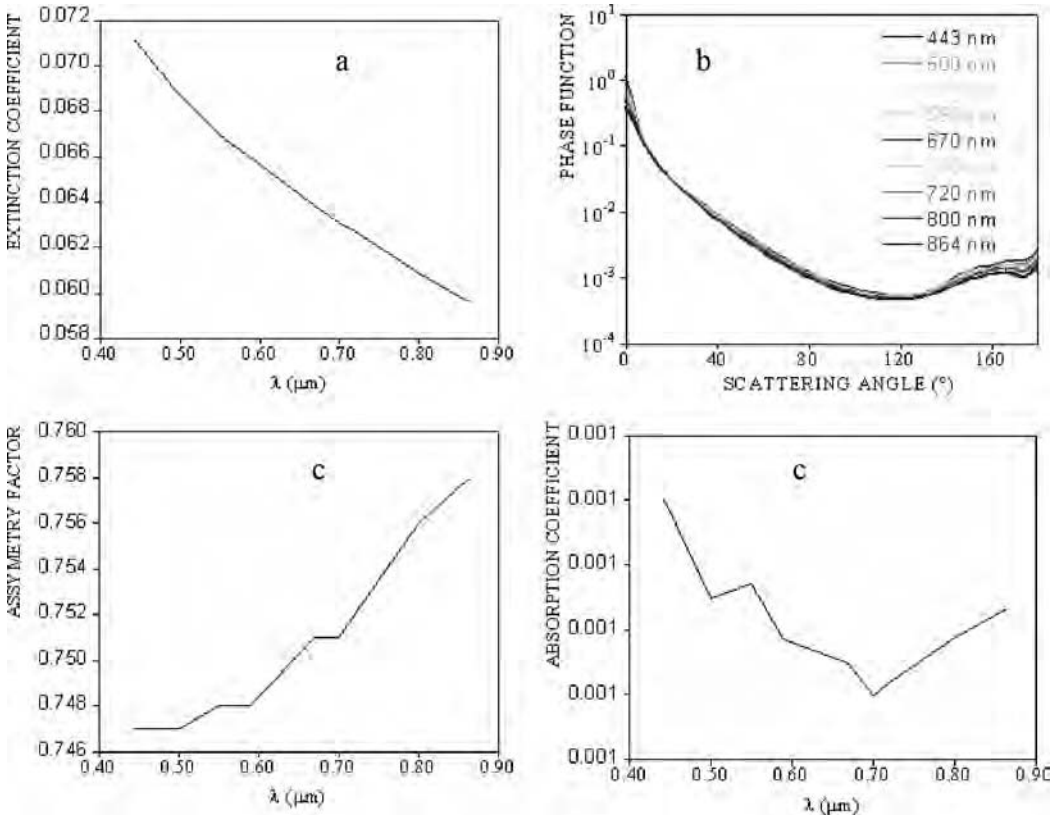

Figure 8. Other aerosol optical properties retrieved with the algorithm: (a) extinction coefficient; (b) phase function; (c) asymmetry factor; (d) absorption coefficient.

CONCLUSIONS

In this paper we have introduced an algorithm based on Simplex minimization to correct atmospherically hyperspectral and multiangular data, paying particular emphasis to aerosols.

The algorithm we have developed is remarkably sensitive to the first guess values of the parameters that are used in the inversion, so a good guess is needed. We have related this fact to another possible solution to the ill-posed problem. The closer we are to reality for the first guess, the more likely we retrieve the solution.

If we intend to use the algorithm for satellite data, the use of the AERONET network would be more suitable, as it provides a global scale for the aerosol properties. Nevertheless the available AERONET information is meteorology maps that only cover AOD at 500 nm and Angstrom Exponent. Thus, it should be necessary further work to use AERONET information in the algorithm.

ACKNOWLEDGEMENTS

This project was funded by the ESA project "Scientific Analysis of the ESA Airborne Multi-Annual Imaging Spectrometer Campaign" through the contract ESTEC 15343/01/NL/MM. R.P. acknowledges Dai Villaescusa comments and suggestions.

BIBLIOGRAPHY

Air Force Research Lab, Space Vehicles Directorate 1999. MODTRAN4 Radiative Transfer Code, http://www.vs.afrl.af.mil/Division/VSBYB/modtran4.html.

ANDERSON, S. M. and K. MAUERSBERGER (1992), Measurements of ozone absorption cross section in the Chappuis band. *Geophysical Research Letters*, 19, 933-936.

BERGER, M., MORENO J., MUELLER A., BEISL U., RICHTER R., SCHAEPMAN M.,

STRUB G., STOLL M.P., NERRY F., LEROY M., RAST M., WURSTEISEN P., and ATTEMA E. 2001. The DAISEX campaigns in Support of a Future Land Surface Processes Mission, *European Space Agency Bulletin, 105*, 101-111.

BODHAINE, B. A., WOOD N. B., DUTTON E. G., and SLUSSER J. R (1999), On Rayleigh optical depth calculations, *Journal of Atmospheric and Oceanic Technology, 16*, 1854-1861.

DESCHAMPS, P. Y., BREON F. M., LEROY M., PODAIRE A., BRICAUD A., J. C. BURIEZ, and SEZE G. 1994. The POLDER Mission: Instrument Characteristics and Scientific Objectives, *IEEE Transactions in Geoscience and Remote Sensing* 32, 598-615.

DRAXLER R.R. 1999. NOAA ARL HYSPLIT MODEL, *NOAA Technical Memorandum ERL ARL 230*.

ESA 2001a. DAISEX (Digital Airborne Imaging Spectrometer Experiment), *European Space Agency Publication Division* SP-499, ESTEC, The Netherlands.

ESA 2001b. Reports for assessment. The Five Candidate Earth Explorer Core Missions: SPECTRA - Surface Processes and Ecosystems Changes Through Response Analysis, *European Space Agency Publication Division*, SP-1257 (5), ESTEC, The Netherlands.

GUEYMARD, C. A. 2001. Parameterized transmittance model for direct beam and circumsolar spectral irradiance, *Solar Energy, 71*, 325-346.

HESS M., KOEPKE P., SCHULTZ I. 1998. Optical properties of aerosol and clouds: the software package OPAC, *Bulletin of the American Meteorological Society*, 79, 5, 831-844.

HOLBEN B.N., ECK T.F., SLUTSKER I. *et al*. 1998. AERONET - A federated instrument network and data archive for aerosol characterization", *Remote Sensing of the Environment,* 66, 1-16.

HOLBEN, B. N., SETZER A., ECK T. F., PEREIRA A., and SLUTSKER I. 1996. Effect of dry season biomass burning on Amazon basin aerosol concentrations and optical properties, 1992-1994, *Journal of Geophysical Research*, 101, 19465-19481.

JAMET C., MOULIN C., THIRIA S. 2004. Monitoring aerosol optical properties over the Mediterranean from SeaWiFS images using a neural network inversion, *Geophysical Research Letters* 31(13), Art. No. L13107.

KASTEN, F. and YOUNG M.T. 1989. Revised optical air mass tables and approximation formula, *Applied Optics, 28*, 4735-4738.

KAUFMAN Y. J., TANRÉ D., REMER L. A., VERMOTE E. F., CHU A. and HOLBEN B. N. 1997. Operational remote sensing of tropospheric aerosol over land from EOS moderate resolution imaging spectroradiometer, *Journal of Geophysical Research*, 102, 17051-17067.

KAUFMAN Y. J. and TANRÉ D. 1996. Strategy for direct and indirect methods for correcting the aerosol effect in Remote Sensing: From AVHRR to EOS-MODIS, *Remote Sensing of the Environment* 55, 67-79.

MARTINEZ-LOZANO J. A., PEDRÓS R., FLAMANT C, UTRILLAS M. P., TENA F., MORENO J., PELON J., CISNEROS J. M. and GONZALEZ-FRIAS C. 2002. a multi-instrument approach for characterizing the atmospheric aerosol optical thickness: case study in the STAARTE/DAISEX99 campaign, *Geophysical Research Letters*, 29(4), 12.1-12.4.

MARTÍNEZ-LOZANO J. A., UTRILLAS M. P., PEDRÓS R., TENA F, DÍAZ J. P., EXPÓSITO F. J., LORENTE J., DE CABO X., CACHORRO V., VERGAZ R. and CARREÑO V. 2003. Intercomparison of spectroradiometers for global and direct solar irradiance in the visible range, *Journal of Atmospheric and Oceanic Technology*, 20, 7, 997-1010.

NAKAJIMA T., TONNA G., RAO R., BOI P., KAUFMAN Y. and HOLBEN B. 1996. Use of sky brightness measurements from ground for remote sensing of particulate polydispersions, *Applied Optics* 35(15), 2675-2686.

NOAA (2005), http://www.arl.noaa.gov/ready/hysplit4.html.

PEDRÓS R. 2001. Determination of aerosol optical properties from solar radiation extinction measurements, *PhD Thesis*, University of Valencia (in Spanish).

PEDRÓS R., MARTÍNEZ-LOZANO J. A., UTRILLAS M. P., GÓMEZ-AMO J.L. and TENA F. 2003. Column-integrated aerosol optical properties from ground-based spectroradiometer measurements at Barrax (Spain) during DAISEX (Digital Airborne Spectrometer Experiment) campaigns, *Journal of Geophysical Research*, 108(D18), Art. No. 4571, doi:10.1029/2002JD003331.

RAHMAN, H., VERSTRAETE M. M., and PINTY B. 1993. Coupled surface-atmosphere reflectance (CSAR) model. 1. Model description and inver-

sion on synthetic data, *Journal of Geophysical Research*, 98, 20,779-20,789.

REMER, L.A. and KAUFMAN Y.J. 1998. Dynamic aerosol model: Urban/industrial aerosol, *Journal of Geophysical Research,* 103, 13859-13871.

REMER, L. A., KAUFMAN Y. J. and HOLBEN B.N. 1999. Interannual variation of ambient aerosol characteristics on the coast of the United States, *Journal of Geophysical Research, 104*, 2223-2231.

ROTHMAN L. S., RINSLAND C. P., GOLDMAN A., *et al.* 1998. The HITRAN molecular spectroscopic database and HAWKS (HITRAN Atmospheric Workstation): 1996 edition, *Journal of Quantitative Spectroscopy and Radiative Transfer* 60 (5): 665-710. HITRAN Database access via <http://cfa-www.harvard.edu/HITRAN>

SANTER R., CARRÈRE V., DESSAILLY D., DUBUISSON P. and ROGER J. C. 1997. Atmospheric corrections over land MERIS level 2 Algorithms Theoretical Basis Document, pp 15-1 to 15-87.

SCHROEDER T. H., FISCHER J., SCHAALE M. and FELL F. 2002. Artificial neural network based atmospheric correction algorithm: Application to MERIS data, in *Proceedings of the International Society for Optical Engineering (SPIE)*, Vol. 4892, Hangzhou, China.

List of abbreviations

AOD – Aerosol Optical Depth.

ARAT – Avion de Recherche Atmosphérique et Télédétection (Remote Sensing and Atmospheric Research Aircraft).

ARL – Air Resources Laboratory.

BRDF – Bidirectional Reflectance Distribution Function.

DAIS – Digital Airborne Imaging Spectrometer.

DAISEX - Digital Airborne Imaging Spectrometer Experiment.

DLR – Deutches Zentrum für Luft- und Raumfahrt e.V. (German Space Agency).

ESA – European Space Agency.

GMT – Greenwich Meridian Time.

HITRAN - HIgh-resolution TRANsmission molecular absorption database

HyMap™ – Hyperspectral Mapping Trade Mark.

HYSPLIT4 – Hybrid Single-Particle Langrangian Integrated Trajectory Model Version 4.

LEANDRE - Lidar Embarqué pour l'étude de l' Atmosphère: Nuages, Dynamique, Rayonnement et cycle de l'Eau (Airborne Lidar to study the atmosphere: clouds, dynamics, radiation and water cycle).

MERIS – Medium Resolution Imaging Spectrometer.

MODTRAN - MODerate spectral resolution atmospheric TRANSsmittance algorithm and computer model.

NOAA – National Oceanic and Atmospheric Administration.

OPAC – Optical Properties of Aerosols and Clouds.

POLDER - POLarization and Directionality of the Earth's Reflectances.

RPV - Rahman-Pinty-Verstraete.

RMBD - Relative Mean Bias Deviation .

RTE – Radiative Transfer Equation.

SeaWiFS - Sea-viewing Wide Field of view Sensor.

SMARTS2 – Simple Model of the Atmosphere Radiative Transfer of Sunshine Version 2.

WSS - Weighted Sum of Squares.